Am J Transl Res 2024;16(6):2190-2211
www.ajtr.org /ISSN:1943-8141/AJTR0155669

Original Article

Integrating network pharmacology with experimental validation to investigate the mechanism of Wuwei Zishen formula in improving perimenopausal syndrome

Xuewen Fu[1], Hui Wang[2], Meichen Gai[3], Yuanhua Dai[3], Jun Chang[3], Hong Zhang[3]

[1]Changchun University of Chinese Medicine, Changchun 130117, Jilin, China; [2]The Affiliated Hospital to Changchun University of Chinese Medicine, Changchun 130021, Jilin, China; [3]Guang'anmen Hospital, China Academy of Chinese Medical Sciences, Beijing 100053, China

Received January 28, 2024; Accepted May 22, 2024; Epub June 15, 2024; Published June 30, 2024

Abstract: Objectives: To investigate the role of the Wuwei Zishen formula (WWZSF) in treating and preventing perimenopausal syndrome (PMS) and to understand its mechanism. Methods: Network pharmacology and molecular docking was used to predict active compounds, potential targets, and pathways for PMS treatment using WWZSF. Female Sprague-Dawley (SD) rats were induced with D-galactose (D-gal) to establish a PMS model and treated with Kunbao pill (KBP) and WWZSF. Estrus cycles were observed using vaginal smears. Serum sex hormones were measured using the enzyme-linked immunosorbent assay (ELISA). Histological changes in the uterus and ovaries were evaluated using hematoxylin-eosin staining (HE). Western blot was used to assess the protein expression levels of Cleaved Caspase-3, p62, BAX/Bcl-2, p-PI3K/PI3K, p-AKT/AKT, and p-mTOR/mTOR in the uterus and ovaries. Results: A total of 70 active compounds and 440 potential targets were screened out. Important targets and pathways, including AKT1, Bcl-2, Caspase-3, mTOR, and the PI3K/AKT/mTOR pathways, and molecular docking verified their high affinities to key WWZSF components. In vivo experiments showed that WWZSF can ameliorate the morphological abnormalities of the uterus and ovaries, increase sex hormone levels and organ index, and restore the estrus cycles in PMS rats. Moreover, the western blot results showed decreased Cleaved Caspase-3 and BAX/Bcl-2 protein levels in the ovarian and uterine tissues after WWZSF therapy. Concurrently, there was an increase in the expression of p62 and the ratios of p-AKT/AKT, p-mTOR/mTOR, and p-PI3K/PI3K. Conclusion: The PI3K/AKT/mTOR signaling pathway-mediated apoptosis and autophagy pathways may be how WWZSF efficiently reduces PMS.

Keywords: Network pharmacology, molecular docking, perimenopausal syndrome, D-galactose, PI3K/AKT/mTOR signaling pathway

Introduction

Perimenopausal syndrome (PMS) refers to a collection of physiological and physical changes in specific organs or tissues resulting from reduced levels of estrogen both before and following the cessation of female reproductive function. PMS can present symptoms such as hot flashes, sweating, menstrual disorders, irritability, and depression. In the absence of prompt and efficient therapy, there can be a significant rise in the risk of postmenopausal osteoporosis, coronary heart disease, and diabetes [1]. The Society for International Menopause reports that Menopausal symptoms are estimated to impact about 1 billion individuals worldwide, with an annual predicted increase of approximately 47 million [2, 3]. Numerous fields, including endocrinology, psychology, and gerontology, are involved in PMS research, making it a primary global public health concern.

Rather than slowing the aging process, PMS treatment aims to enhance women's health and quality of life by alleviating various painful symptoms [4]. Although hormone therapy can effectively improve vasomotor symptoms and urogenital tract atrophy, it requires a comprehensive assessment of the patient's age, health status, and risk of complications. The risk-to-benefit ratio of hormone therapy is still contro-

https://doi.org/10.62347/RQHY5963

versial [5]. Therefore, developing precise, efficient, and less side-effect non-hormone therapy medications is a crucial and continuing research area that will support the advancement of menopausal women's health [6]. Hormone replacement therapy for PMS has been a part of Traditional Chinese Medicine (TCM) for thousands of years. Its benefits for early management, apparent long-term efficacy, and reduced side effects to ameliorate PMS have been demonstrated in numerous clinical practices [7-9]. Additionally, examining the mechanism by which TCM treats PMS unveiled its capacity to regulate endocrine hormone levels, promote ovarian proliferation, and impede endometrium cell apoptosis [10, 11]. Due to the many prescriptions and complex components of TCM, there is a diversity of perspectives on the efficacy of TCM in disease treatment. Hence, more research is needed to determine the mechanism of these drugs.

The ingredients of the Wuwei Zishen formula (WWZSF) were: Schisandrae Chinensis Fructus (Wu Wei Zi), Leonuri Herba (Yi Mu Cao), Fructus Tritici Levis (Fu Xiao Mai), Mori Follum (Sang Ye), Cinnanmomi Cortex (Rou Gui), and Ecliptae Herba (Mo Han Lian). Pharmacological investigation demonstrates that Schisandrae Chinensis Fructus can alleviate menopausal symptoms, particularly hot flashes, sweating, and palpitations [12]. Leonuri Herba has anti-aging and anti-inflammatory qualities [13]. Fructus Tritici Levis has an evident antiperspirant action, which differs from wheat [14]. Mori Follum and Cinnanmomi Cortex can suppress fat, decrease blood sugar, stimulate glucose metabolism, and improve obesity [15, 16]. Ecliptae Herba's potent ingredients can treat osteoporosis, strengthen bones, and suppress the production of osteoclasts [17]. Clinical research demonstrates that WWZSF, a novel Chinese medicine mixture, can raise hormone levels in PMS sufferers and alleviate hot flashes, as well as decrease sweating, general upset, follicle depletion, and other symptoms. However, further investigation into its mechanisms of action is necessary due to its intricate composition and unknown pharmacological processes.

Using big data technologies, and network pharmacology, a breakthrough paradigm in drug research reveals the systemic and molecular underpinnings of TCM, transforming the discipline from experience-based to evidence-based medicine [18, 19]. Network pharmacology allows us to construct a "Herbs-Ingredients-Targets-Disease" network in order to elucidate the mechanisms of action for specific drugs. Molecular docking techniques can study the interaction between small molecule ligands and protein receptors. The combination of the two can help us to design and develop new drugs [20].

In this work, we used network pharmacology to anticipate the primary targets and signal pathways of WWZSF and confirmed it in vivo experiments, which provided a foundation for clinical use of WWZSF.

Material and methods

Screening the active components in WWZSF

The Traditional Chinese Medicine Systems Pharmacology Database and Analysis Platform (TCMSP) database (https://old.tcmsp-e.com/tcmsp.php) was searched to find the active components of WWZSF and the related in vivo target proteins. The active components in the database were screened based on two criteria: drug-likeness (DL) ≥ 0.18 and oral bioavailability (OB) ≥ 30%. Among these, the chemical composition of Fructus Tritici Levis was ascertained by a review of the literature [14]. The PubChem database collected the simplified molecular input line entry system (SMILES) chemical expression of active compounds (https://pubchem.ncbi.nlm.nih.gov/). To predict the corresponding gene name of each component, it was entered into the Swiss Target Prediction database (http://www.swisstargetprediction.ch/). The research subject was limited to "Homo sapiens" for screening, and remaining parameters were kept as default. Finally, we merged and eliminated duplicate targets to get the dataset.

Collection of PMS targets

The keywords "perimenopause syndrome", "menopause syndrome", "menopause", and "climacteric" were used to search in the Genecards (http://www.genecards.org/), Disgenet (https://www.disgenet.org/) and OMIM (www.omim.org/) databases. When searching the Disgenet database for keywords, matching synonyms were selected. All PMS-related genes

were obtained in the three databases and exported to excel to remove duplicates.

Obtaining intersection genes

The targets of WWZSF and PMS were mapped in the Microbioinformatics resource (http://www.bioinformatics.com.cn/), and a Venn diagram was generated to get the intersection genes.

Building "Herbs-Ingredients-Targets-Disease" network

The "Herbs-Ingredients-Targets-Disease" network diagram was designed using Cytoscape 3.9.1 bioinformatics analysis software and analysed using the CytoNCA plug-in, which was loaded with the intersection targets and active components of WWZSF.

Building protein-protein interaction (PPI) network

All intersection genes were uploaded into the STRING database (https://string-db.org/). Selected the research species as "Homo sapiens" and set the confidence interval of correlation ≥ 0.900. The remaining parameters were kept as default. For topological attribute analysis, we imported the relevant tsv format files into Cytoscape 3.9.1 software, then used the CytoNCA plug-in to calculate the PPI network degree values and created a visual PPI network diagram with high degree values.

Gene Ontology (GO) and Kyoto Encyclopedia of Genes Genomes (KEGG) enrichment analysis

For GO and KEGG function enrichment analysis, the intersection genes were added to the Metascape web platform (http://metascape.org/). "Homo sapiens" was selected as the species. The top 20 results of KEGG and top 15 results of GO were selected for visualization, and bubble diagrams were used to display the enrichment results.

Molecular docking

The ligand's three-dimensional (3D) structures were downloaded from the PubChem database (https://pubchem.ncbi.nlm.nih.gov/). For the molecular optimization procedure, SYBYL-X 2.0 was employed. The 3D structure of the receptor was ascertained using the RCSB database (http://www.rcsb.org). Using the MGLTools1.5.6 program, the receptors were fixed and processed (i.e., water molecules and metal ions were removed) before being saved as a pdbqt file. The AutoDock Vina1.1.2 program (http://vina.scripps.edu/) evaluates the target proteins' propensity for docking with components. Discovery Studio was used to finish the final graphical display of the molecular docking data.

Reagents and drugs

WWZSF consisted of Schisandrae Chinensis Fructus (21 g), Mori Follum (21 g), Fructus Tritici Levis (12 g), Leonuri Herba (9 g), Ecliptae Herba (9 g), and Cinnanmomi Cortex (2 g). The Jilin Academy of Traditional Chinese Medicine (Jilin, China) provided all the above drugs. The six herbs mentioned above are cooked 3 times in water, the first time, decocted with 10 times the volume of water for 1.5 hours, then another 8 times the volume for the second and third times, decocted for 1.5 hours each time. Finally, the concentration of WWZSF solution is 0.55 g/mL. D-galactose (D-gal) was acquired from Shanghai McLean Biochemical Technology Co., Ltd. (Shanghai, China; lot: D810318). Kunbao pill (KBP) was purchased from Beijing Tong Ren Tang Co., Ltd. (Beijing, China; lot: Z11020185). The Nanjing Jiancheng Bioengineering Institute in Jiangsu, China, is the source of the enzyme-linked immunosorbent assay (ELISA) kits for luteinizing hormone (LH), follicle-stimulating hormone (FSH), and estradiol (E_2). These antibodies were used: anti-phospho (p)-62, anti-Cleaved Caspase-3, anti-PI3K, anti-p-PI3K, and anti-AKT (Cell Signaling Technology, Danvers, USA); goat anti-rabbit and goat anti-mouse (Beyotime Biotechnology, Shanghai, China); anti-BAX, anti-Bcl-2, anti-GAPDH, anti-p-AKT, anti-mTOR and anti-p-mTOR (Proteintech, Rosemont, USA).

Animal source

Twelve week old female SD rats weighing 275±10 g (SYXK (JI) 2018-0001) were obtained from Changchun Yisi Experimental Animal Technology (Jilin, China). The rats were provided access to food and water, and their housing was maintained at a constant temperature of 22°C with a 12-hour light/dark cycle. This study was approved by the Institutional Review Board of the College of Basic Medical Sciences, Jilin University, China (No. 2022-398) before the experiment.

Animal model establishment and treatment

Four groups (n = 10) consisting of forty female SD rats with regular estrous cycles were randomly assigned: Control group, D-gal group, KBP group, and WWZSF group. Intraperitoneal injections of 0.9% saline were administered to the control group, and intraperitoneal injections of D-gal (450 mg/kg) were administered to the WWZSF, KBP, and D-gal groups. The necessary medication was given via gavage starting from the sixth week. To the "Equivalent dose ratio table converted by body surface area between human and animal", the control and D-gal groups were gavaged with an equivalent volume of normal saline (10 ml/kg), the rats in the KBP and WWZSF groups were administered the KBP suspension (1.0 g/kg) and WWZSF suspension (14.8 g/kg) respectively. Every group received a four-week supply of gavage treatments.

Estrus cycle

Daily between 9 and 10 am, a pipette gun was used to gently aspirate a small amount of saline (0.9% NaCl) and introduce it into the rat vagina for repeated blowing. A drop of suspension was then gathered on a slide, allowed to dry, and dyed with gentian violet [21]. An optical microscope was then used to assess the cell morphology. Cell types in vaginal exfoliated cell smears were used to determine the duration of the estrous cycle in rats. Many nucleated epithelial cells and a low percentage of cornified epithelial cells were visible in the proestrus visual field. Cornified epithelial cells with uniform staining constituted most cell types during the estrus phase. Among the cell types observed in metestrus are leukocytes, nucleated epithelial cells, and cornified epithelial cells. Leukocytes predominated in the diestrus visual field, with few cornified epithelial cells remaining visible [22].

General condition and organ index

During the experiment, we carefully observed the overall characteristics of each group of rats, such as their body weight, the glossiness and softness of their fur, their degree of activity, and their mental condition. Twenty-four hours after the last dose, all rats were anesthetized and then blood directly from the heart was collected. After that, animals were euthanized by carbon dioxide inhalation. Then the uterus and ovaries were removed and weighed (wet weight). Organ index (mg/g) = Organ weight (mg) times body weight (g) × 100%.

ELISA

ELISA assays were employed to quantify E_2, FSH, and LH levels. The detection procedures were conducted per the instructions provided by the kit, and the test was performed.

Hematoxylin-eosin (HE) staining

The ovaries and uterus tissues were first fixed using a 4% paraformaldehyde solution and then washed with running water. Subsequently, the tissues were dehydrated, waxed, embedded, and solidified. They were then sliced into 4 μm thick slices, stained with hematoxylin-eosin, and viewed under an optical microscope.

Western blot

Proteins were extracted from the ovarian and uterine tissue samples using a radioimmunoprecipitation assay (RIPA) lysis buffer. Proteins were separated on sodium dodecyl sulfate-polyacrylamide gel electrophoresis (SDS-PAGE) (New Cell & Molecular Biotech, Jiangsu, China) and transferred on poly-vinylidene fluoride (PVDF) membranes. The PVDF membrane was sealed tightly for 1.5 hours at room temperature using skimmed milk powder. Subsequently, it was treated with secondary antibodies for 2 hours at room temperature, following an overnight incubation at 4°C with primary antibodies. Protein bands were identified using electrochemical luminescence (ECL) reagents, and the bands were observed using Syngene Bio Imaging (Synoptics, Cambridge, UK).

Statistical analysis

All data were presented as the mean ± standard deviation. The data from the two groups were analyzed with one-way of variance (ANOVA) test and data followed a normal distribution. GraphPad Prism version 8.3.0 statistical software was used to create analyses and graphics. A value of $P < 0.05$ was considered significant.

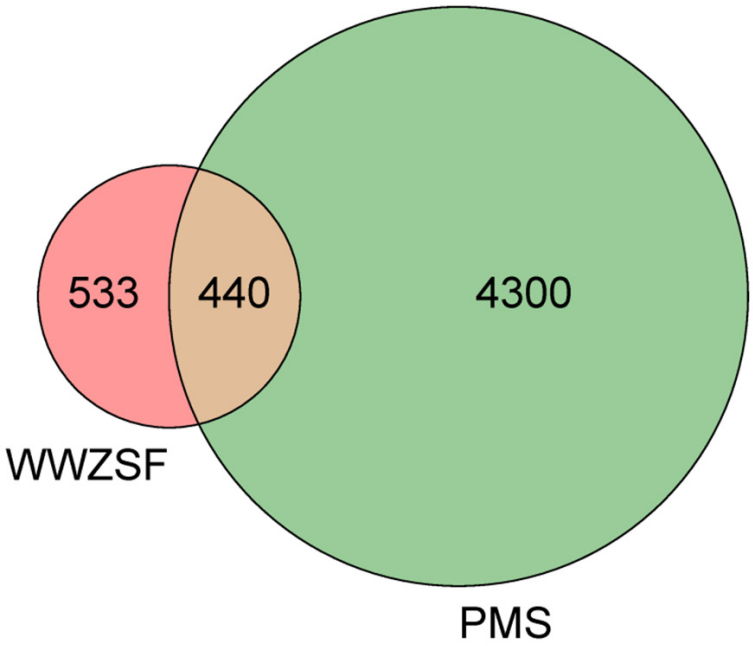

Figure 1. Venn diagram was visualized to analyze the common potential targets of perimenopausal syndrome (PMS) and Wuwei Zishen formula (WWZSF).

Results

Active ingredients and targets of action of WWZSF

A total of 70 active components were screened by TCMSP database, comprising 8 from Schisandrae Chinensis Fructus, 29 from Mori Follum, 10 from Ecliptae Herba, 8 from Leonuri Herba, and 10 from Cinnanmomi Cortex. By reviewing the literature, 5 valuable components of Fructus Tritici Levis were identified [14]. Swiss Target Prediction database was used to convert the target names acquired from TCMSP into human genes. After the process of merging and de-duplicating, a total of 973 target genes were finally obtained.

Gene targets for PMS

A total of 4271, 528, and 12 PMS-related targets were obtained from three databases, GeneCards, OMIM, and DisGenet, respectively. A total of 4740 disease targets were acquired after eliminating duplicate targets.

Construction of Venn diagrams

The WWZSF and PMS targets were mapped to obtain 440 intersection targets, that is, the potential target for WWZSF to improve PMS (**Figure 1**).

"Herbs-Ingredients-Targets-Disease" interaction

The "Herbs-Ingredients-Targets-Disease" diagram was created using the Cytoscape 3.9.1 program to investigate the pharmacological mechanism of WWZSF (**Figure 2**). The network consists of 518 nodes and 4376 edges, red circular nodes represent WWZSF and PMS, green hexagonal nodes in the middle represent potential targets of WWZSF in treating PMS, the surrounding octagonal and diamond nodes in different colors represent Mori Follum (Sang Ye), Schisandrae Chinensis Fructus (Wu Wei Zi), Leonuri Herba (Yi Mu Cao), Fructus Tritici Levis (Fu Xiao Mai), Cinnanmomi Cortex (Rou Gui), Ecliptae Herba (Mo Han Lian) and their potent components. The 4376 purple edges represent the interaction between WWZSF active ingredients and PMS. According to the CytoNCA plug-in in Cytoscape 3.9.1 software, the degree value of the node was obtained. A higher the degree value of the node indicates a higher number of the nodes associated with it. Among the most crucial components are Pratensein, Albanol, Iristectorigenin A, 5-Nonadecylresorcinol, 3'-O-Methylorobol, Tetramethoxy luteolin, and Schizandrer B. **Table 1** presents the findings.

PPI network

A total of 440 overlapping targets were uploaded to the STRING online platform to obtain PPI network data, which were imported into Cytoscape 3.9.1 to draw a PPI network diagram including 48 nodes and 1023 edges. The CytoNCA plug-in in Cytoscape 3.9.1 was used to calculate the degree value of PPI network, including degree value, betweenness centrality and closeness centrality. The degree value is reflected by the size and color of the target points (**Figure 3**). Among them, protein kinase B (AKT1), tumor protein p53 (TP53), interleukin 6 (IL-6), tumor necrosis factor (TNF), epidermal

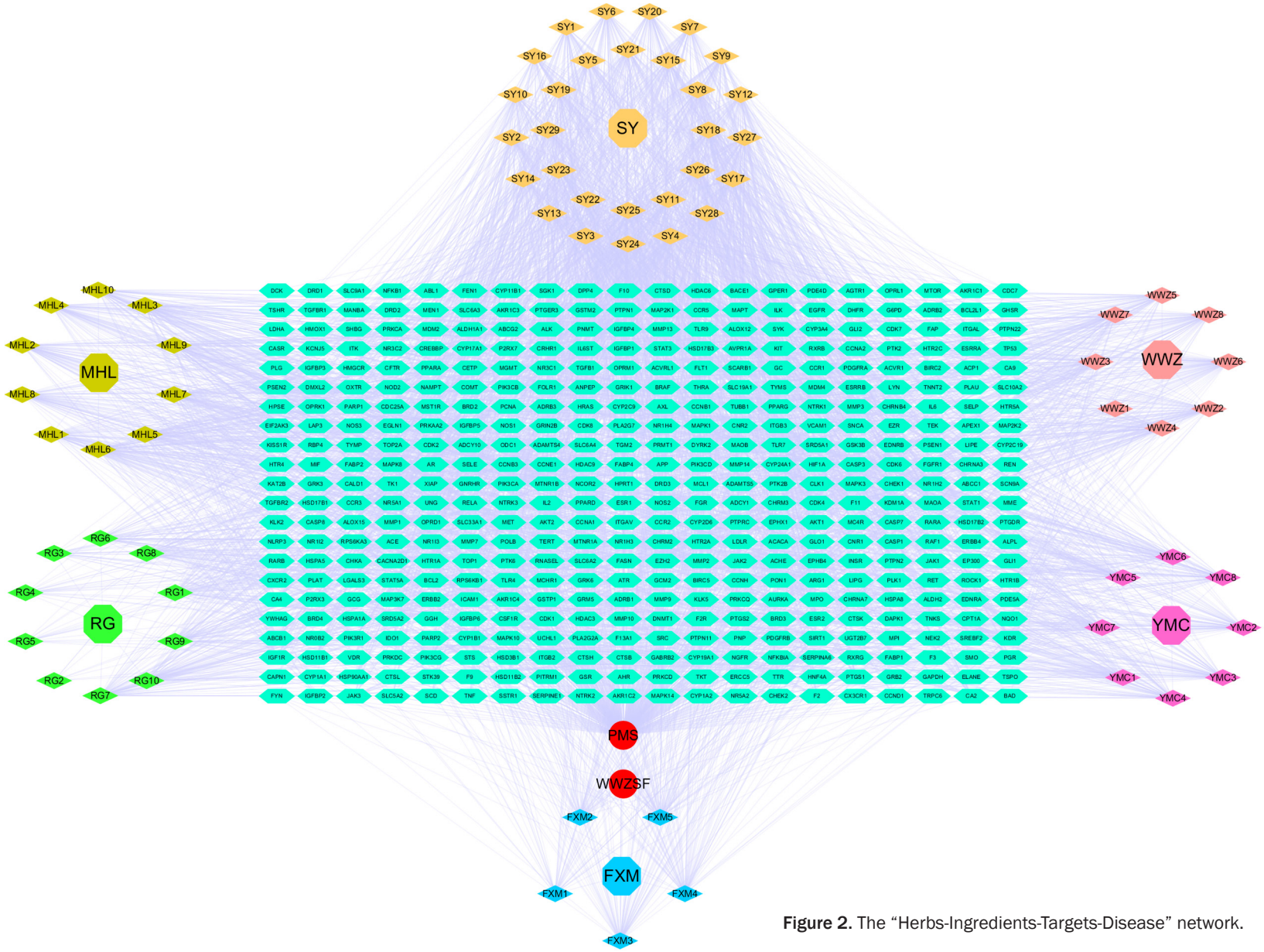

Figure 2. The “Herbs-Ingredients-Targets-Disease” network.

Table 1. Results of degree values of Wuwei Zishen formula (WWZSF) active ingredients in the "Herbs-Ingredients-Targets-Disease" network

Chinese name NO.	Latin name	Ingredient	Degree
Mo Han Lian 6	Ecliptae Herba	Pratensein	71
Sang Ye 4	Mori Follum	Albanol	69
Sang Ye 24	Mori Follum	Iristectorigenin A	69
Fu Xiao Mai 3	Fructus Tritici Levis	5-Nonadecylresorcinol	68
Mo Han Lian 5	Ecliptae Herba	3'-O-Methylorobol	67
Sang Ye 28	Mori Follum	Tetramethoxyluteolin	67
Wu Wei Zi 4	Schisandrae Chinensis Fructus	Schizandrer B	66
Fu Xiao Mai 4	Fructus Tritici Levis	5-Heneicosylresorcinol	66
Wu Wei Zi 2	Schisandrae Chinensis Fructus	Deoxyharringtonine	65
Wu Wei Zi 6	Schisandrae Chinensis Fructus	Gomisin G	64
Fu Xiao Mai 5	Fructus Tritici Levis	5-Pentacosyl-1,3-benzenediol	64
Mo Han Lian 7	Ecliptae Herba	Demethylwedelolactone	64
Sang Ye 11	Mori Follum	Moracin E	64
Sang Ye 17	Mori Follum	Oxysanguinarine	64
Sang Ye 25	Mori Follum	Icosa-11,14,17-trienoic acid methyl ester	64
Wu Wei Zi 8	Schisandrae Chinensis Fructus	Wuweizisu C	63
Mo Han Lian 3	Ecliptae Herba	Butin	63
Mo Han Lian 9	Ecliptae Herba	Luteolin	63
Sang Ye 7	Mori Follum	Isoramanone	63
Sang Ye 9	Mori Follum	Moracin C	63
Sang Ye 12	Mori Follum	Moracin F	63
Sang Ye 27	Mori Follum	Linolenic acid ethyl ester	63
Mo Han Lian 2	Ecliptae Herba	Acacetin	62
Mo Han Lian 4	Ecliptae Herba	1,3,8,9-tetrahydroxybenzofurano[3,2-c]chromen-6-one	62
Mo Han Lian 10	Ecliptae Herba	Quercetin	62
Sang Ye 6	Mori Follum	26-Hydroxy-dammara-20,24-dien-3-one	62
Sang Ye 18	Mori Follum	Quercetin	62
Sang Ye 20	Mori Follum	Kaempferol	62
Sang Ye 26	Mori Follum	Norartocarpetin	62
Yi Mu Cao 2	Leonuri Herba	Kaempferol	62
Yi Mu Cao 3	Leonuri Herba	Quercetin	62
Yi Mu Cao 4	Leonuri Herba	Isorhamnetin	62
Sang Ye 8	Mori Follum	Moracin B	61
Yi Mu Cao 8	Leonuri Herba	β-Sitosterone	61
Mo Han Lian 8	Ecliptae Herba	Wedelolactone	60
Sang Ye 15	Mori Follum	4-Prenylresveratrol	60
Wu Wei Zi 5	Schisandrae Chinensis Fructus	Angeloylgomisin O	59
Rou Gui 7	Cinnanmomi Cortex	(-)-Caryophyllene oxide	59
Sang Ye 21	Mori Follum	Stigmasterol	59
Rou Gui 10	Cinnanmomi Cortex	Oleic acid	58
Sang Ye 5	Mori Follum	Inophyllum E	58
Wu Wei Zi 7	Schisandrae Chinensis Fructus	Gomisin R	57
Mo Han Lian 1	Ecliptae Herba	Linarin	57
Rou Gui 9	Cinnanmomi Cortex	(-)-α-cedrene	57
Sang Ye 1	Mori Follum	Poriferast-5-en-3β-ol	57
Sang Ye 19	Mori Follum	β-sitosterol	57
Sang Ye 16	Mori Follum	FA	56
Sang Ye 10	Mori Follum	Moracin D	55
Wu Wei Zi 3	Schisandrae Chinensis Fructus	Angeloylgomisin O	54

Rou Gui 1	Cinnanmomi Cortex	EIC	54
Sang Ye 2	Mori Follum	Scopolin	54
Yi Mu Cao 5	Leonuri Herba	Iso-preleoheterin	54
Yi Mu Cao 6	Leonuri Herba	Preleoheterin	54
Fu Xiao Mai 2	Fructus Tritici Levis	Allantoin	53
Sang Ye 29	Mori Follum	Skimmin (8Cl)	53
Sang Ye 13	Mori Follum	Moracin G	51
Sang Ye 14	Mori Follum	Moracin H	51
Sang Ye 22	Mori Follum	Arachidonic acid	51
Sang Ye 23	Mori Follum	Supraene	51
Yi Mu Cao 1	Leonuri Herba	Arachidonic acid	51
Yi Mu Cao 7	Leonuri Herba	Galeopsin	51
Rou Gui 8	Cinnanmomi Cortex	DIBP	50
Sang Ye 3	Mori Follum	Carotene	50
Rou Gui 6	Cinnanmomi Cortex	()-Ledene	49
Fu Xiao Mai 1	Fructus Tritici Levis	Carotene	41
Rou Gui 3	Cinnanmomi Cortex	β-carotene	25
Rou Gui 4	Cinnanmomi Cortex	Junipene	21
Rou Gui 5	Cinnanmomi Cortex	()-Sativene	15
Rou Gui 2	Cinnanmomi Cortex	()-Aromadendrene	8
Wu Wei Zi 1	Schisandrae Chinensis Fructus	Longikaurin A	5

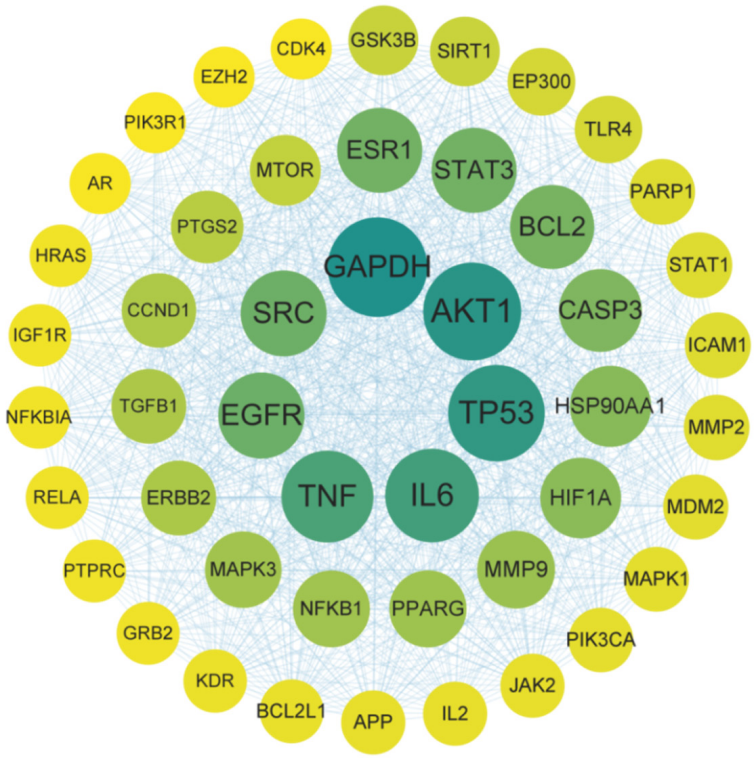

Figure 3. Protein-protein interaction (PPI) network diagram.

growth factor receptor (EGRF), sarcoma gene (SRC), estrogen receptor 1 (ESR1), signal transducer and activator of transcription 3 (STAT3), B-cell lymphoma-2 (Bcl-2), and Caspase-3 (CASP3) of WWZSF acting in PMS targets had high degree value, suggesting that these target proteins may be crucial targets for WWZSF treatment of PMS. The parameters related to the core target network with the top 20 degree values are listed in **Table 2**.

GO and KEGG enrichment analysis

GO and KEGG enrichment analyses were conducted utilizing the Metascape platform to investigate the critical biological processes and signaling pathways involved in treating PMS with WWZSF. **Figure 4** displays the top 15 items for the GO analysis of biological processes (BP), cellular components (CC), and molecular function (MF). These items regulate hormone levels, membrane valves, protein kinase complexes, adhesion spots, and protein kinase activity. Moreover, multiple KEGG pathways, including path-

Table 2. The top 20 core targets and information of protein-protein interaction (PPI) network

Target gene	Degree	Betweenness Centrality	Closeness Centrality
GAPDH	260	0.0610	0.712
AKT1	253	0.0420	0.704
TP53	247	0.0457	0.695
IL6	235	0.0411	0.684
TNF	228	0.0337	0.678
EGFR	204	0.0237	0.652
SRC	203	0.0544	0.648
STAT3	199	0.0145	0.645
ESR1	199	0.0354	0.647
BCL2	195	0.0145	0.642
CASP3	190	0.0131	0.637
HSP90AA1	183	0.0207	0.630
HIF1A	181	0.0113	0.629
MMP9	169	0.0138	0.615
PPARG	166	0.0207	0.617
NFKB1	165	0.0065	0.613
MAPK3	164	0.0137	0.614
ERBB2	157	0.0112	0.607
TGFB1	156	0.0103	0.604
CCND1	155	0.0076	0.603

ways in cancer, Chemical carcinogenesis-receptor activation, PI3K/AKT signaling pathway, Hepatitis B, and Prostate cancer, could play important roles in treating PMS by WWZSF (**Figure 5**). Based on the close relationship between the PI3K/AKT signaling pathway and PMS, the PI3K/AKT signaling pathway was chosen as the signaling pathway to explore its mechanism in this study.

Docking of molecules

Using KEGG enrichment analysis, the PI3K/AKT signaling pathway associated with apoptosis was identified. The PPI network examined AKT1, Bcl-2, Caspase-3, and mTOR as key proteins in the pathway connected to apoptosis. The binding activity of significant targets and critical active components of WWZSF was identified using molecular docking studies (**Table 3**). Better binding between the compound and the target is often indicated by a binding energy of less than -7.0 kcal/mol. AKT1, Caspase-3, mTOR, and PI3K are all well-combined with each other from the perspective of the target. Tetramethoxyluteolin and 3'-O-Methylorobol attach to each target more effectively when viewed from the component perspective (**Figure 6**). Therefore, our results offer theoretical backing for the targeting of WWZSF in managing PMS, which is linked to regulating apoptosis and the PI3K/AKT/mTOR signaling cascade.

WWZSF shortens the estrous cycle in PMS rats

We assessed rat vaginal exfoliated cell smears to illustrate further the contribution of WWZSF to enhancing reproductive endocrinology in PMS. Compared to the control group, the rats in the D-gal group had an irregular estrous cycle and a prolonged diestrus cycle during the last week of the study. Rats' estrous cycles were restored to normal and were shortened to five days after receiving KBP and WWZSF treatments (**Figure 7**).

WWZSF improves appearance, body weight, ovarian weight, and ovarian index in PMS rats

Rats in the D-gal intraperitoneally showed yellow, dry-knotted fur that was sparse, listless, as well as decreased activity compared to the control group (**Figure 8A**). Weekly weighing records indicated an initial decline in the rats' weight after the start of modeling, that was followed by a gradual increase. By the end of the experiment, no statistical differences in weight were observed between the groups (**Figure 8B**). Compared with the control group, the ovarian weight and ovarian index in the D-gal group were decreased, and the ovarian wet weight and ovarian index were increased after KBP and WWZSF intervention. There was a statistically significant difference in the KBP group (**Figure 8C-E**).

WWZSF increases hormone levels in PMS rats

Serum E_2 levels were considerably lower in the D-gal group compared to the control group. In contrast, FSH and LH levels were significantly increased, consistent with PMS hormone alterations. Following medication intervention, there was a noticeable decrease in FSH and LH levels and a significant increase in serum E_2 levels in the KBP and WWZSF groups. This suggests that WWZSF can efficiently raise PMS rats' hormone levels (**Figure 9**).

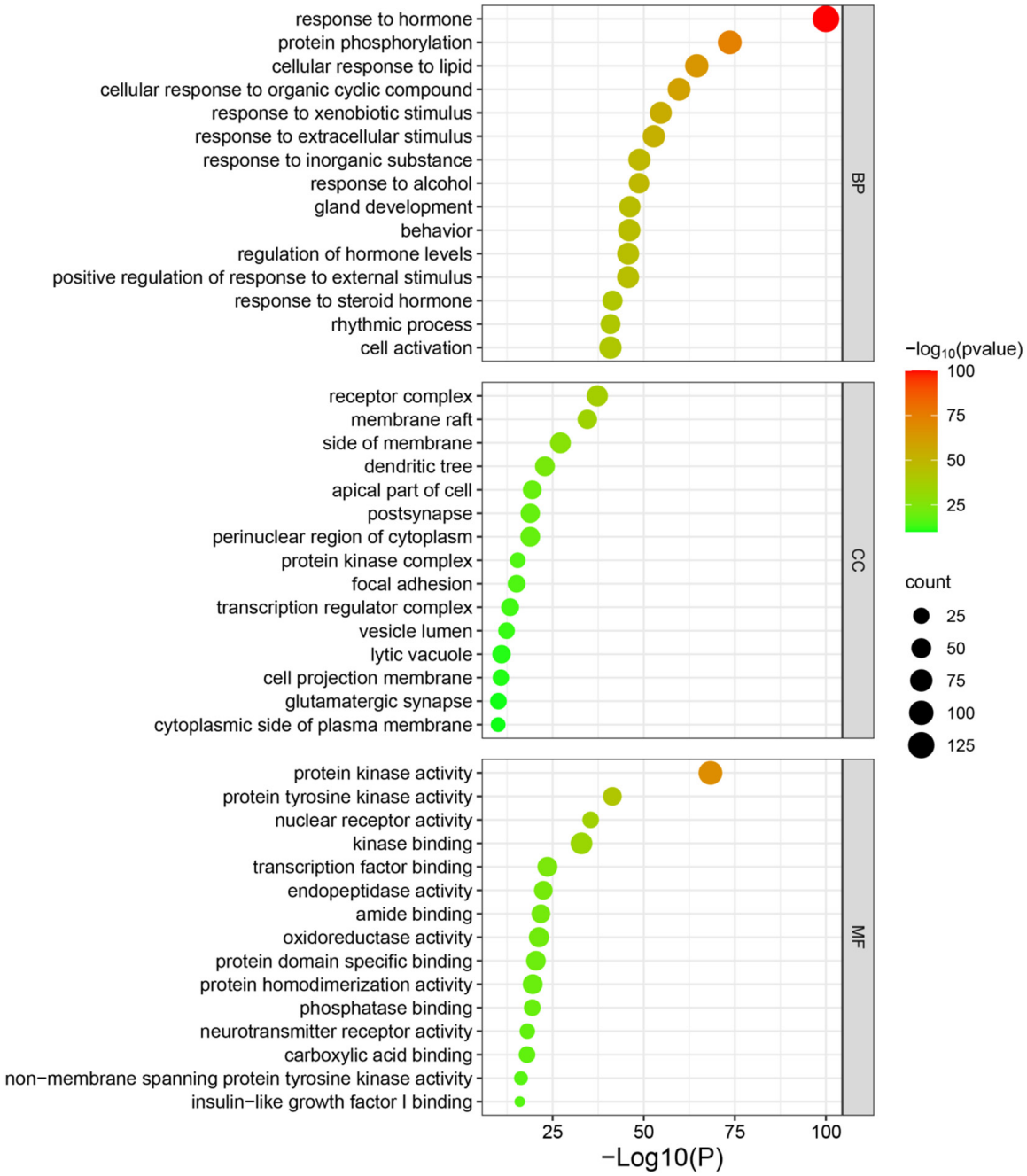

Figure 4. Top 15 results of Biological processes (BP), cellular components (CC) and molecular function (MF) of Gene Ontology (GO) enrichment analysis.

WWZSF ameliorated ovarian pathology in PMS rats

Histopathological observations revealed fewer dominant follicles, corpora lutea, and fewer granulosa cells in the PMS group than in the control group. However, these histopathological characteristics could be improved by drug intervention. The KBP group exhibited suboptimal dominant follicle development, characterized by fewer follicles. The development of the luteum was significant and distinguished by an increased size and densely packed granular cells. In the WWZSF group, mature follicles had a significant amount of follicular fluid, the corpus luteum was of substantial size, and the

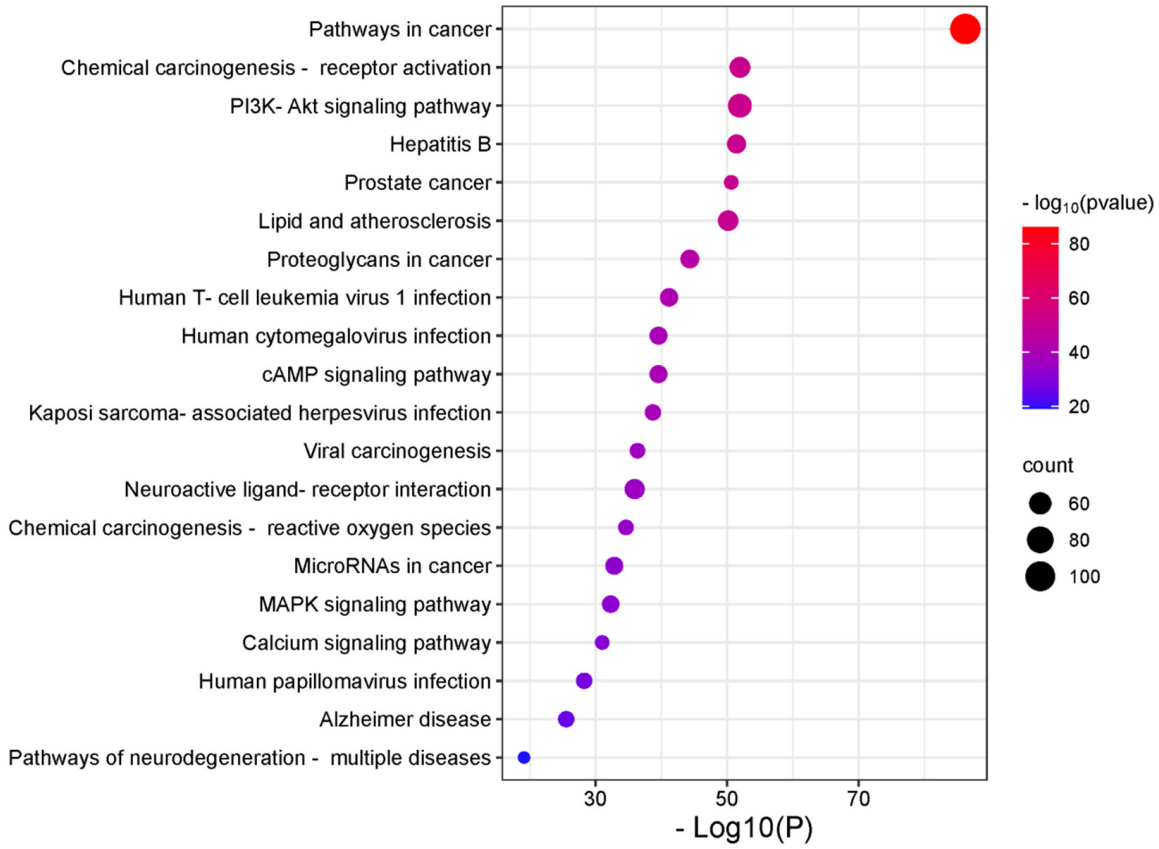

Figure 5. Top 20 results of Kyoto Encyclopedia of Genes and Genomes (KEGG).

Table 3. Molecular docking of targets and primary active components

Ingredient	Bcl-2	Caspase-3	PI3K	AKT1	mTOR
3'-O-Methylorobol	-7.6	-7.9	-8	-9.5	-9.2
Pratensein	-6.4	-7.8	-8.2	-9.3	-9.2
Iristectorigenin A	-6.2	-7.8	-7.8	-9.2	-7.8
Tetramethoxyluteolin	-7.3	-8	-8.1	-9.1	-8.1
Schizandrer B	-6.1	-7.3	-9	-7.8	-9

granular cells were organized in multiple layers and exhibited tidiness (**Figure 10**).

WWZSF inhibits ovarian tissue apoptosis

We used the western blot technique to verify ovarian tissue apoptosis in order to confirm our theory. The expression of Cleaved Caspase-3 protein and the ratio of BAX/Bcl-2 in the ovaries of D-gal rats were considerably higher than those of the control group. KBP and WWZSF treatment suppressed apoptosis of the ovaries, as evidenced by the downregulation of the Cleaved Caspase-3 protein expression and the BAX/Bcl-2 ratio (**Figure 11**).

WWZSF regulates the PI3K/AKT/mTOR signaling pathway

The KEGG analysis and molecular docking results conclude that a key signal pathway through which WWZSF influences PMS is the PI3K/AKT/mTOR pathway. Western blot analysis showed that the ratio of p-PI3K/PI3K, p-AKT/AKT, and p-mTOR/mTOR were significantly downregulated in the ovarian tissue of the PMS rats compared with that in the control group, at the same time, WWZSF treatment upregulated the level of these ratios. This indicates that in PMS-induced ovarian tissues in rats, WWZSF can activate the PI3K/AKT/mTOR signaling pathway (**Figure 12**).

WWZSF prevents the overactivation of autophagy

It was examined whether D-gal might activate autophagy and how WWZSF affected autophagy in order to learn more about the possible

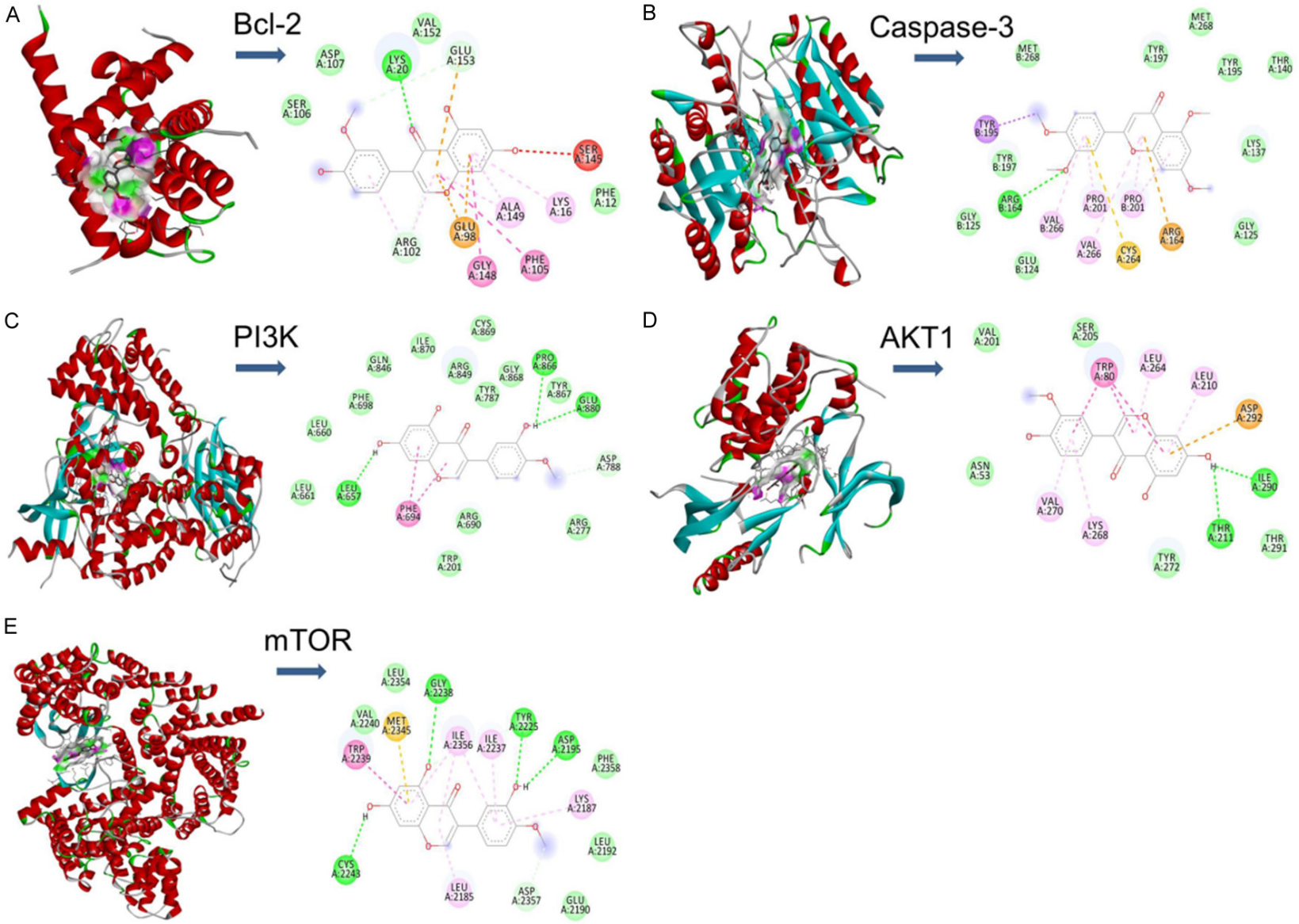

Figure 6. Molecular docking. A. 3'-O-Methylorobol and Bcl-2. B. Tetramethoxyluteolin and Caspase-3. C. Pratensein and PI3K. D. 3'-O-Methylorobol and AKT1. E. Pratensein and mTOR.

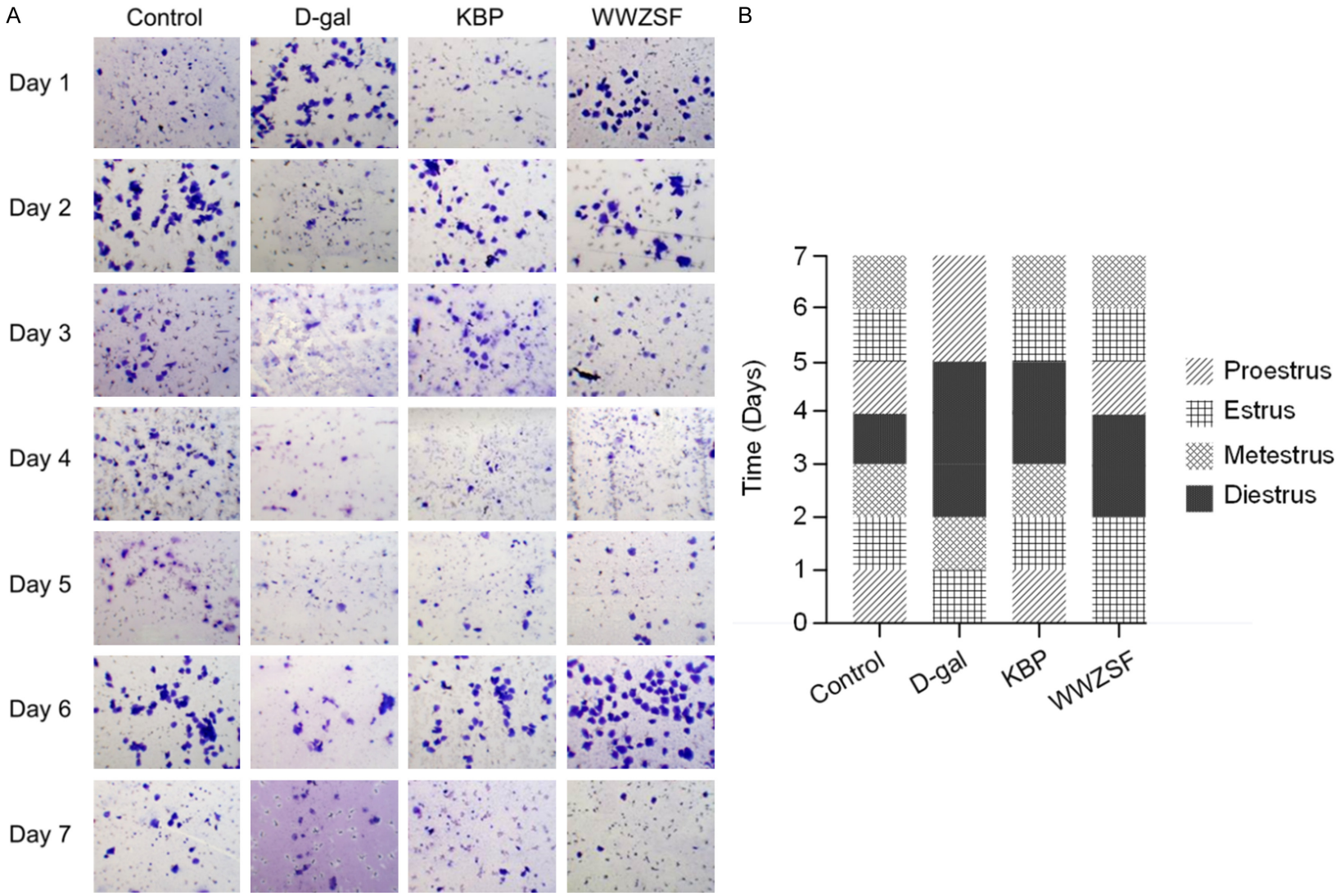

Figure 7. The rat estrus cycle in the last week of the experiment. A. Rat vaginal exfoliated cells stained with crystal violet solution (×40). B. The estrous cycle statistics table.

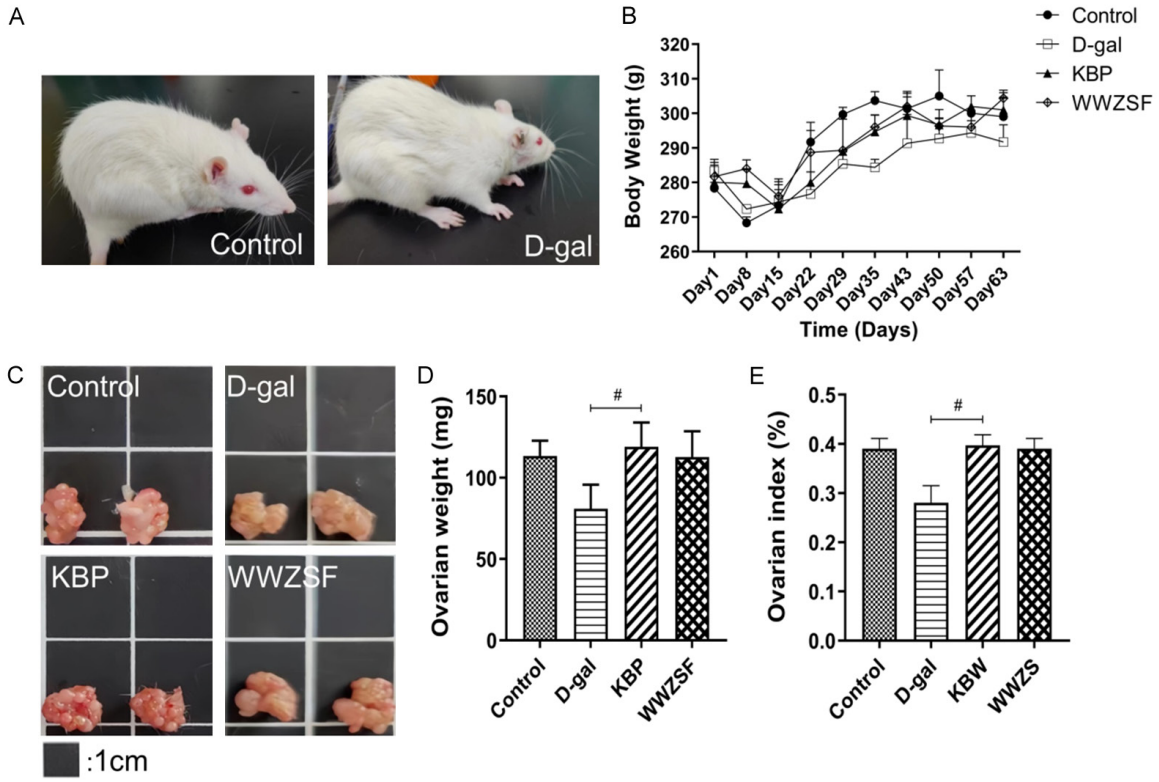

Figure 8. WWZSF improved the appearance, weight, apparent morphology of ovarian tissue, ovarian weight, and ovarian index of PMS rats. A. Shift in the appearance of the model rats. B. Body weight. C. Apparent morphology of ovarian tissue. D. Ovarian weight. E. Ovarian index. Data are presented as mean ± SD, n = 3. $^{\#}P < 0.05$ vs. D-gal.

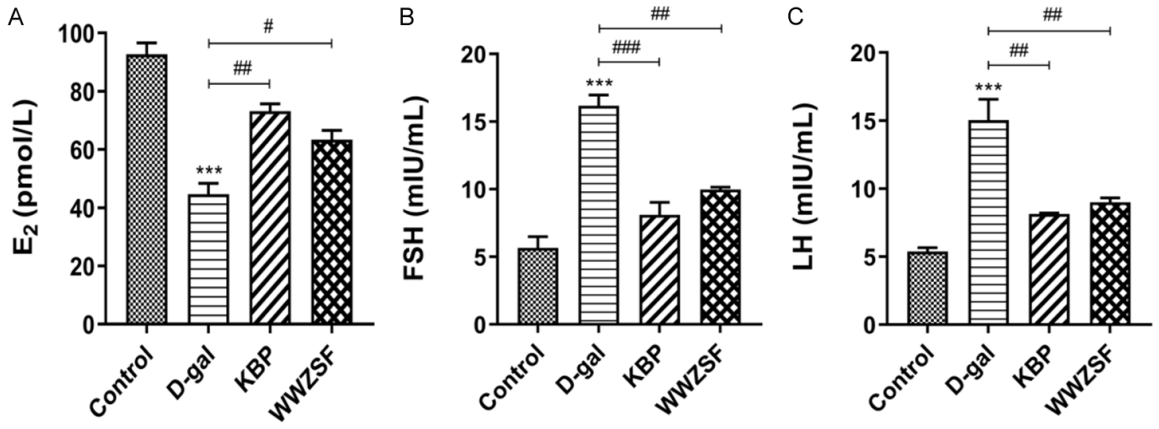

Figure 9. Effects of WWZSF on the sex hormone levels in PMS rats. A. Estradiol (E_2). B. Follicle-stimulating hormone (FSH). C. Luteinizing hormone (LH). Data are presented as mean ± SD, n = 3. $^{***}P < 0.001$ vs. control; $^{\#}P < 0.05$ vs. D-gal, $^{\#\#}P < 0.01$ vs. D-gal, $^{\#\#\#}P < 0.001$ vs. D-gal.

mechanism by which it reduces PMS. The expression of p62 protein in the ovary was detected by Western blot. **Figure 13** demonstrated that p62 protein expression was significantly reduced in the D-gal group compared to the control group, whereas KBP and WWZSF can dramatically increase p62 expression.

WWZSF promoted uterus weight and uterus index in PMS rats

We further evaluated the uterine weight and index to study the therapeutic effect of WWZSF on the uterus. Rats in the D-gal group showed a substantial drop in wet weight and uterine

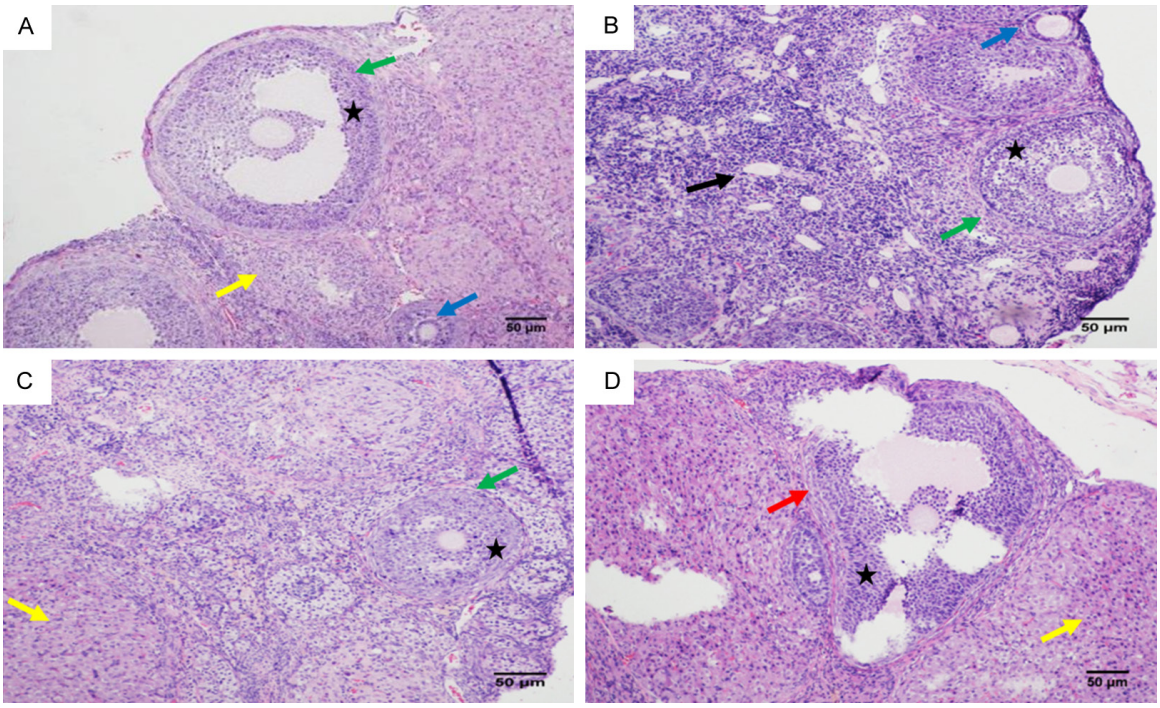

Figure 10. Effects of WWZSF on the pathological morphology of ovarian tissue observed by Hematoxylin-Eosin staining. A. Control group. B. D-gal group. C. KBP group. D. WWZSF group. Blue →: Primary follicles. Green →: Secondary follicles. Red →: Mature follicles. Black →: Atretic follicles. Yellow →: Corpus luteum. ★: Ovarian granular cells. Bar = 50 μm.

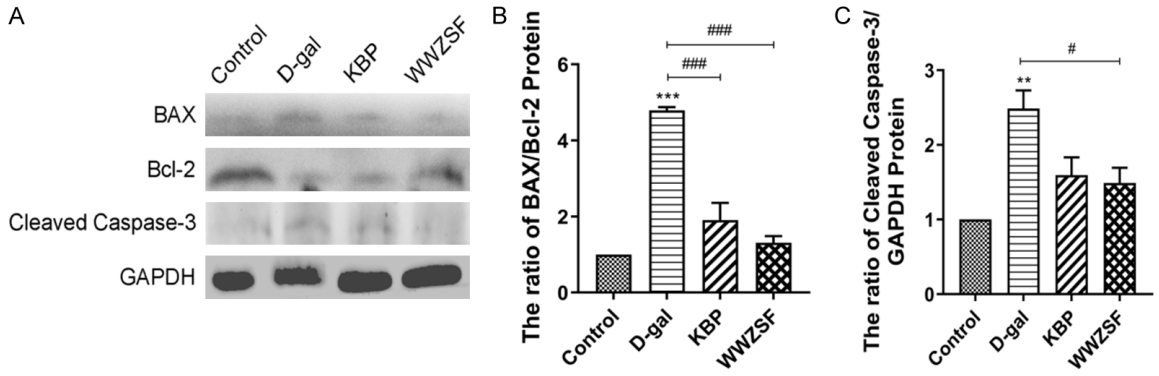

Figure 11. Expression of apoptosis-related proteins in ovaries tissues of rats in different groups. A. The protein bands of BAX, Bcl-2, and Cleaved Caspase-3 were detected by Western Blot. B. Quantitative analysis of expression levels of BAX/Bcl-2. C. Quantitative analysis of expression levels of Cleaved Caspase-3. Data are presented as mean ± SD, n = 3. $^{**}P < 0.01$ vs. control, $^{***}P < 0.001$ vs. control; $^{\#}P < 0.05$ vs. D-gal, $^{\#\#\#}P < 0.001$ vs. D-gal.

index as compared to the control group, but the WWZSF group showed a significant increase in both metrics (**Figure 14**).

WWZSF ameliorated uterine pathology in PMS rats

HE staining results of uterine tissue showed that in the control group, the endometrium was thicker, and uterus glands were abundant. In the D-gal group, the endometrium was thinner, the number of uterus glands decreased, and the whole uterus was in a state of atrophy. After KBP intervention, there was a moderate improvement in the quantity of endometrium and glands. After WWZSF intervention, the endometrium of rats thickened, and the number of glands increased (**Figure 15**).

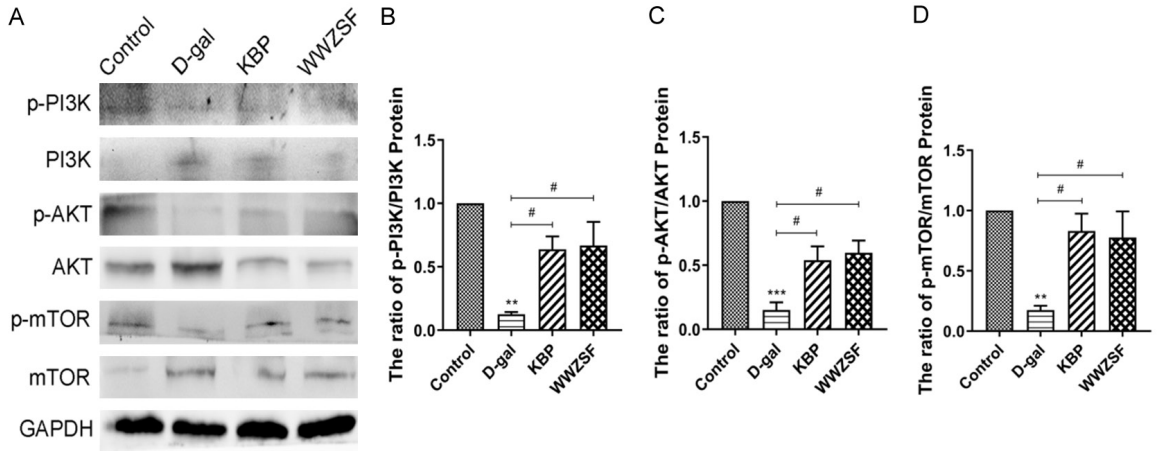

Figure 12. Expression of PI3K/AKT/mTOR signaling pathway related proteins in ovaries tissues of rats in different groups. A. The protein bands of p-PI3K, PI3K, p-AKT, AKT, p-mTOR, and mTOR were detected by Western Blot. B. Quantitative analysis of expression levels of p-PI3K/PI3K. C. Quantitative analysis of expression levels of p-AKT/AKT. D. Quantitative analysis of expression levels of p-mTOR/mTOR. Data are presented as mean ± SD, n = 3. $^{**}P < 0.01$ vs. control, $^{***}P < 0.001$ vs. control; $^{\#}P < 0.05$ vs. D-gal.

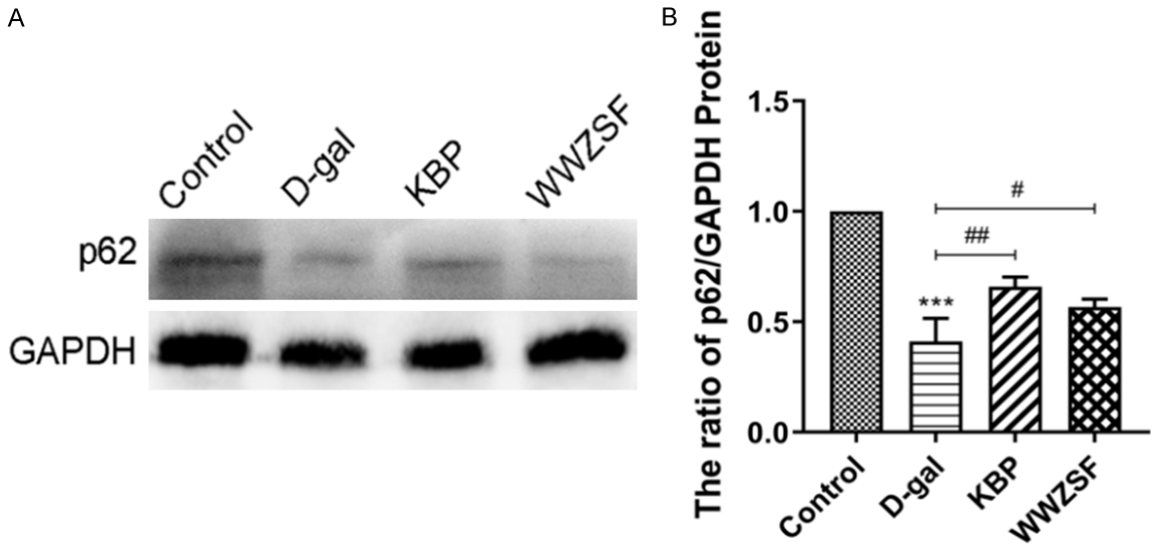

Figure 13. Expression of p62 protein in ovaries tissues of rats in different groups. A. The protein band of p62 was detected using Western Blot. B. Quantitative analysis of expression levels of p62. Data are presented as mean ± SD, n = 3. $^{***}P < 0.001$ vs. control; $^{\#}P < 0.05$ vs. D-gal, $^{\#\#}P < 0.01$ vs. D-gal.

WWZSF activates the PI3K/AKT/mTOR signaling pathway to prevent uterine apoptosis and autophagy

Western blot results in uterine tissue similarly demonstrated that following intraperitoneal injection of D-gal, there was an increase in the expression of pro-apoptosis-related proteins Cleaved Caspase-3 and BAX/Bcl-2, a decrease in the ratio of p-PI3K/PI3K, p-AKT/AKT, p-mTOR/mTOR and a significant decrease in the expression of p62 protein. On the other hand, the WWZSF gavage treatment increased the expression of p62 protein, p-PI3K/PI3K, p-AKT/AKT, p-mTOR/mTOR ratio, and decreased the BAX/Bcl-2 ratio. It also suppressed the expression of the Cleaved Caspase-3 protein. The uterine results align with ovarian findings, suggesting that WWZSF can inhibit apoptosis and autophagy, counteract D-gal-induced endometrial atrophy, increase the number of uterine glands, and restore uterine function. These

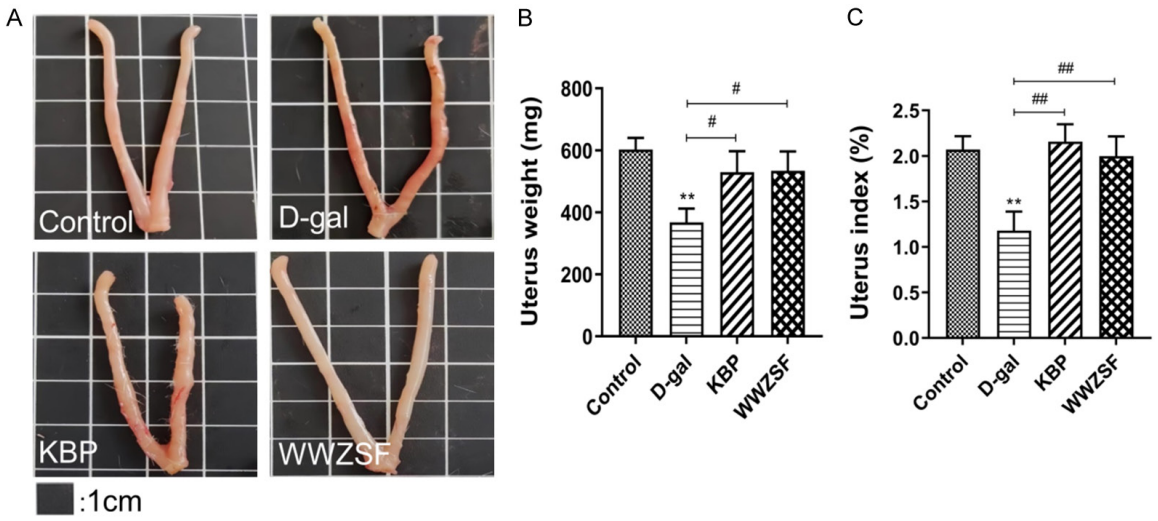

Figure 14. WWZSF improved the apparent morphology of uterine tissue, uterine weight, and uterine index of PMS rats. A. Morphology of uterus. B. Uterus weight. C. Uterus index. $^{**}P < 0.01$ vs. control; $^{\#}P < 0.05$ vs. D-gal, $^{\#\#}P < 0.01$ vs. D-gal.

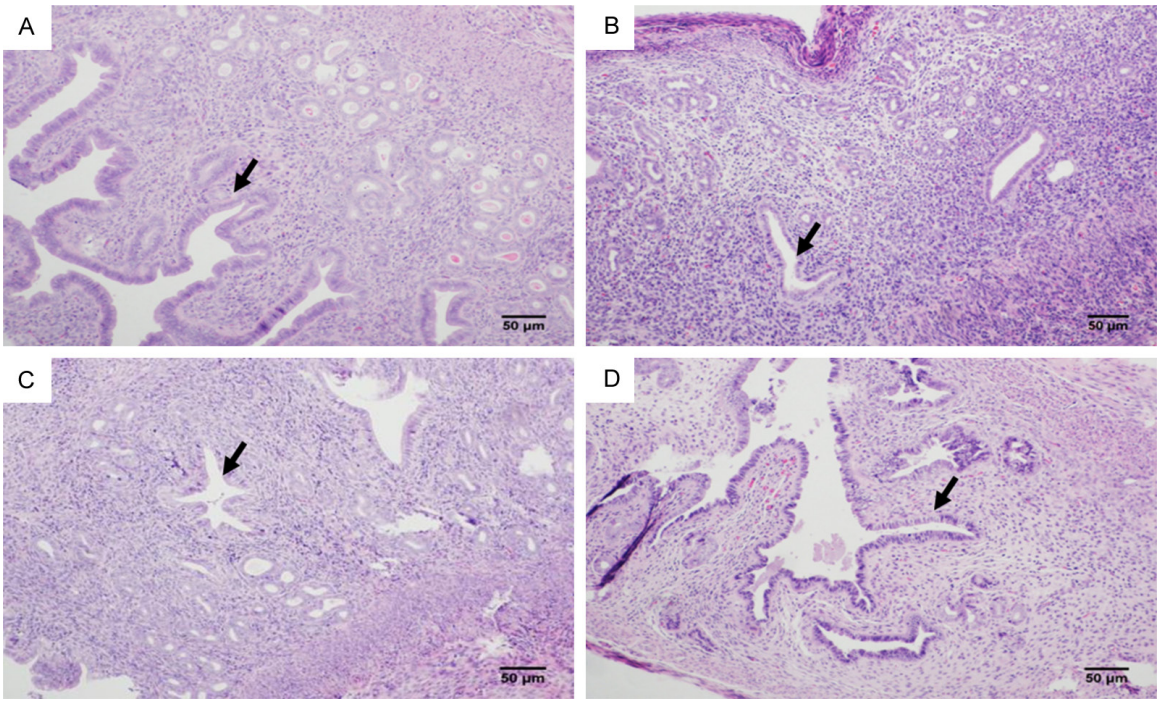

Figure 15. Effects of WWZSF on the pathological morphology of uterine tissue observed by Hematoxylin-Eosin staining. A. Control group. B. D-gal group. C. KBP group. D. WWZSF group. Black →: Uterine gland. Bar = 50 μm.

effects appear to be mediated by the activation of the PI3K/AKT/mTOR signaling pathway (**Figure 16**).

Discussion

The incidence rate of PMS is on the rise, with a younger tendency, owing to the aging process and the pace of life, in contrast to the general extension of life and the increased concern of the entire society for physical and mental health [23]. Low estrogen levels and ovarian function decline are closely related to the occurrence of the PMS. During the perimenopause era, the number of primordial follicles

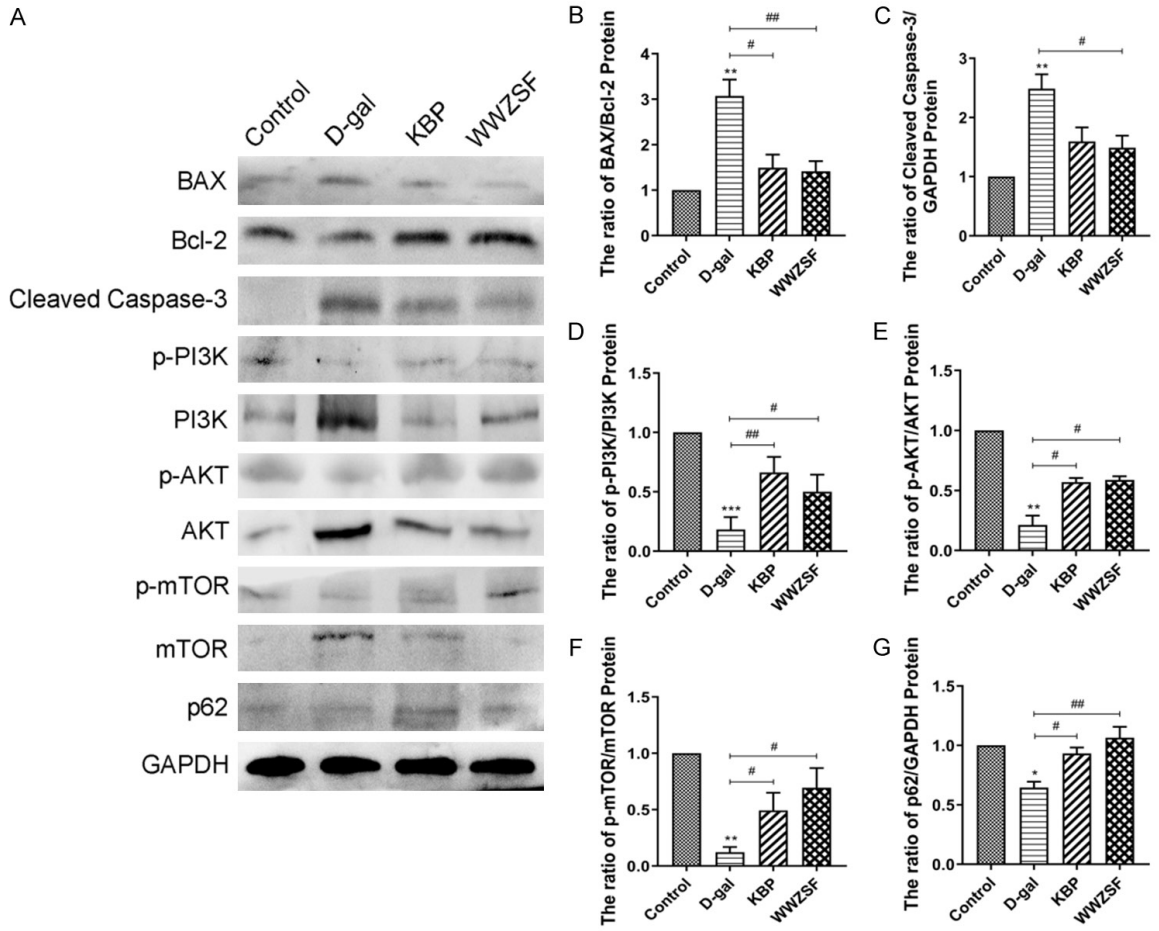

Figure 16. Expression of key proteins in uterus tissues of rats in different groups. A. The protein bands of BAX, Bcl-2, Cleaved Caspase-3, p-PI3K, PI3K, p-AKT, AKT, p-mTOR, mTOR, and p62 were detected by Western Blot. B. Quantitative analysis of expression levels of BAX/Bcl-2. C. Quantitative analysis of expression levels of Cleaved Caspase-3. D. Quantitative analysis of expression levels of p-PI3K/PI3K. E. Quantitative analysis of expression levels of p-AKT/AKT. F. Quantitative analysis of expression levels of p-mTOR/mTOR. G. Quantitative analysis of expression levels of p62. Data are presented as mean ± SD, n = 3. $^{*}P < 0.05$ vs. control, $^{**}P < 0.01$ vs. control, $^{***}P < 0.001$ vs. control; $^{\#}P < 0.05$ vs. D-gal, $^{\#\#}P < 0.01$ vs. D-gal.

and mature follicles decreased, the secretion of E_2 decreased, and the level of FSH increased. The balance of sex hormones becomes off at this point. The endometrium became thinner, and the uterine atrophies under low estrogen [24, 25]. Consequently, a new line of inquiry of study is to examine the synergistic effects of TCM substances and the essential therapy processes. In this study, we used network pharmacology and animal research to explore the complex active components and modes of action of WWZSF in D-gal-induced PMS modeled rats.

Network pharmacology is a novel approach in TCM research that uses biological network information databases and computer technology to establish and examine the relationships between drugs, proteins, and diseases [26]. In this study, the main active compounds used by the network to treat PMS are Pratensein, Albanol, Iristectorigenin A, 3'-O-Methylorobol, Tetramethoxyluteolin, and Schizandrer B. Previous studies indicate that these active ingredients are lignin and flavonoids, which are naturally occurring anti-aging substances with anti-inflammatory and anti-apoptotic properties that can effectively treat age-related degenerative disorders [27-29]. Schizandrer B is extracted from Schisandrae Chinensis Fructus, Iristectorigenin A and Tetramethoxyluteolin are extracted from Mori Follum, Pratensein and 3'-O-Methylorobol are extracted from Ecliptae

Herba. The sovereign medicines, Schisandrae Chinensis Fructus and Mori Follum are used to nourish kidney yin. Ecliptae Herba as a minister medicine can nourish yin and regulate menstruation. They are consistent with the WWZSF principle. This also demonstrates that the WWZSF treatment of PMS results from the combined action of numerous active ingredients. In addition, enrichment analysis on 440 intersecting targets revealed that WWZSF was involved in regulating the hormone levels, response to protein phosphorylation, and activating protein kinases. The treatment of WWZSF may also influence some cell components and molecular functions, including membrane rafts, sides of the membrane, dendritic trees and protein binding. Enrichment analysis showed that the PI3K/AKT signaling pathway was evidently enriched and closely related to the PMS. The critical target proteins AKT1, Bcl-2, Caspase-3, and mTOR in the PI3K/AKT/mTOR signaling pathway were found by PPI network analysis. Through molecular docking, it was confirmed that the core proteins of Bcl-2, Caspase-3, and PI3K/AKT/mTOR pathways had good binding ability with the above key compounds. This suggested that WWZSF may improve the occurrence of PMS by regulating apoptosis and proliferation through the PI3K/AKT/mTOR pathway.

We chose D-gal, which is stable and potent, as it can accelerate whole body aging in order to better explore the pathological mechanism of PMS. Meanwhile, we chose rats with endocrine changes, reliable reproductive cycles, and better intervention effects on aging for experimental research. Our results demonstrated that D-gal injection can establish the PMS model. WWZSF has a significant effect on PMS modeled in rats, including normalizing the rat status and ovulation cycles, increasing the index of the ovary and uterus, changing the levels of sex hormones, and ameliorating the morphological abnormalities of the ovary and uterus. These results are consistent with previous studies [30].

Apoptosis is an essential mechanism for preserving the stability of the biological environment, especially in ovarian aging. The decline of ovarian function in PMS modeled rats is mainly due to the increase of atresia follicles because of the apoptosis of ovarian granulosa cells. The two main proteins that influence apoptosis are BAX and Bcl-2, which together activate the mitochondrial apoptosis pathway. The downstream executive factor Caspase-3 is then activated via the caspase family cascade response, which eventually results in apoptosis [31, 32]. According to a study, the infusion of the herb decoction increases the expression of Bcl-2, a protein connected to reproduction, it downregulates the expression of the proteins BAX and Caspase-3 in the ovaries, promoting follicular development [33]. In line with the research report, our experiment demonstrated that WWZSF can significantly lower the expression of Cleaved Caspase-3 protein and the ratio of BAX/Bcl-2 in the D-gal group. It can also inhibit apoptosis of the uterus and ovaries to thicken the endometrium and restore normal ovulation caused by D-gal.

Based on network theory research, we hypothesized that the primary pathway by which WWZSF improves PMS is the PI3K/AKT/mTOR signaling pathway. Accumulating data suggest that the PI3K/AKT/mTOR signaling pathway is involved in the physiological and pathological processes of PMS [34]. Shang verified in vivo that ovarian cells can survive longer and that D-gal-induced ovarian decline can be reversed by activating the PI3K/AKT pathway [35]. According to a different study, TCM increases the number of follicles in PMS modeled rats by activating the PI3K/AKT/mTOR signaling pathway [36]. Consistent with these investigations, our results demonstrate that D-gal treated rats have reduced activity of the PI3K/AKT/mTOR signaling pathway, as seen by a drop in the p-PI3K/PI3K, p-AKT/AKT, and p-mTOR/mTOR ratios. WWZSF can upregulate the levels of p-PI3K, p-AKT, and p-mTOR, significantly activating the activity of the PI3K/AKT/mTOR pathway.

Furthermore, impaired autophagy is another sign of aging in tissues, and activation of mTOR can inhibit autophagy [37, 38]. Choi's team demonstrated in vivo that the upstream PI3K/AKT pathway regulates mTOR. This system can be inhibited to promote autophagy through apoptosis and induce follicular atresia [39]. Recent studies have emphasized that ovarian granulosa cells apoptosis is induced by autophagy, and the aggregation of autophagosomes promotes ovarian apoptosis by reducing the

level of Bcl-2 and activating Caspase family [40]. When autophagosomes form, the p62 protein binds to ubiquitinated proteins and fuses with lysosomes to be removed. It is one of the most researched autophagy substrates. Thus, the expression of the p62 protein was also detected by Western blot. The outcomes demonstrated that the D-gal group rat's ovaries and uterus had considerably lower p62 protein expression levels. WWZSF could promote the expression of p62 protein. It is suggested that WWZSF prevents autophagy over-activation and reduces apoptosis in ovarian and uterine tissues through the PI3K/AKT/mTOR signalling pathway [41].

Although the relevant mechanism of WWZSF in treating PMS has been identified in the research mentioned above, there are still several limitations in this study. First, we could not obtain further confirmation of the effects of different WWZSF concentrations through our investigation. The relationship between autophagy and apoptosis has not been fully investigated. Second, we have only used rat PMS models in our in vivo animal tests; future research using human ovarian granulosa cells may be more clinically applicable. Consequently, we intend to conduct additional pertinent research to strengthen our experimental findings.

In summary, our investigation, which combined integrated network pharmacology with experimental validation, found that WWZSF improves PMS by activating the PI3K/AKT/mTOR pathway. This is manifested as a shortened estrus cycle, increased organ index, increased E_2 hormone, decreased FSH and LH hormone, and ameliorated uterine and ovarian tissue morphology. This study provides scientific evidence supporting the use of WWZSF for PMS and suggests a new drug for the treatment of PMS.

Acknowledgements

This study was supported by the Technology Department of Jilin Province, China (20190304073YY).

Disclosure of conflict of interest

None.

Address correspondence to: Hong Zhang, Department of Gynecology, Guang'anmen Hospital, China Academy of Chinese Medical Sciences, No. 5 North Line Pavilion, Xicheng District, Beijing 100053, China. Tel: +86-15801687368; E-mail: zhanghong@ccucm.edu.cn

References

[1] Chen W, Chen M, Tang H, Wei W, Shao P, Dou S, Wu J, Lu B, Shi R and Chen J. Advances in diagnosis and treatment of perimenopausal syndrome. Open Life Sci 2023; 18: 20220754.

[2] Sourouni M, Zangger M, Honermann L, Foth D and Stute P. Assessment of the climacteric syndrome: a narrative review. Arch Gynecol Obstet 2021; 304: 855-862.

[3] Santoro N. Perimenopause: from research to practice. J Womens Health (Larchmt) 2016; 25: 332-339.

[4] Voedisch AJ, Dunsmoor-Su R and Kasirsky J. Menopause: a global perspective and clinical guide for practice. Clin Obstet Gynecol 2021; 64: 528-554.

[5] Pan M, Pan X, Zhou J, Wang J, Qi Q and Wang L. Update on hormone therapy for the management of postmenopausal women. Biosci Trends 2022; 16: 46-57.

[6] Flores VA, Pal L and Manson JE. Hormone therapy in menopause: concepts, controversies, and approach to treatment. Endocr Rev 2021; 42: 720-752.

[7] Wang Y, Lou XT, Shi YH, Tong Q and Zheng GQ. Erxian decoction, a Chinese herbal formula, for menopausal syndrome: an updated systematic review. J Ethnopharmacol 2019; 234: 8-20.

[8] Nguyen TV and Wong FW. The effects of Chinese medicinal herbs on postmenopausal vasomotor symptoms of Australian women. Med J Aust 2001; 175: 230.

[9] Cao XJ, Huang XC and Wang X. Effectiveness of Chinese herbal medicine granules and traditional Chinese medicine-based psychotherapy for perimenopausal depression in Chinese women: a randomized controlled trial. Menopause 2019; 26: 1193-1203.

[10] Wu YY, Li SY, Zhu HQ, Zhuang ZM, Shao M, Chen FL, Liu CS and Tang QF. Network pharmacology integrated with experimental validation reveals the regulatory mechanism of action of Hehuan Yin decoction in polycystic ovary syndrome with insulin resistance. J Ethnopharmacol 2022; 289: 115057.

[11] Guan L, Xue L, Chu J, Xue J, Zhang S and Zhu L. Effect of Tiaojingzhixue Fang on the expression of sex hormone and endometrial tissue mRNA in perimenopausal patients with abnormal uterine bleeding. Cell Mol Biol (Noisy-legrand) 2022; 67: 317-323.

[12] Park JY and Kim KH. A randomized, double-blind, placebo-controlled trial of Schisandra chinensis for menopausal symptoms. Climacteric 2016; 19: 574-580.
[13] Miao LL, Zhou QM, Peng C, Liu ZH and Xiong L. Leonurus japonicus (Chinese motherwort), an excellent traditional medicine for obstetrical and gynecological diseases: a comprehensive overview. Biomed Pharmacother 2019; 117: 109060.
[14] Pei MR, Meng S and Li HF. Comparative study of antiperspirant effect and content of 5-undecylresorcinol and other compounds between floating wheat and wheat. Chinese Archives of Traditional Chinese Medicine 2013; 31: 2030-2032.
[15] Gruenwald J, Freder J and Armbruester N. Cinnamon and health. Crit Rev Food Sci Nutr 2010; 50: 822-834.
[16] Kim DS, Lee HY, Kim HJ, Lee GH, Lim YJ, Ko BM, Kim JH, Kim TW, Kim HK, Kim TY, Hwang DI, Choi HK, Ju SM, Chung MJ and Chae HJ. Combined treatment of mori folium and mori cortex radicis ameliorate obesity in mice via UCP-1 in brown adipocytes. Nutrients 2023; 15: 3713.
[17] Liu YQ, Zhan LB, Liu T, Cheng MC, Liu XY and Xiao HB. Inhibitory effect of Ecliptae herba extract and its component wedelolactone on preosteoclastic proliferation and differentiation. J Ethnopharmacol 2014; 157: 206-211.
[18] Nogales C, Mamdouh ZM, List M, Kiel C, Casas AI and Schmidt HHHW. Network pharmacology: curing causal mechanisms instead of treating symptoms. Trends Pharmacol Sci 2022; 43: 136-150.
[19] Li S and Zhang B. Traditional Chinese medicine network pharmacology: theory, methodology and application. Chin J Nat Med 2013; 11: 110-120.
[20] Saikia S and Bordoloi M. Molecular docking: challenges, advances and its use in drug discovery perspective. Curr Drug Targets 2019; 20: 501-521.
[21] Wang S, Lin S, Zhu M, Li C, Chen S, Pu L, Lin J, Cao L and Zhang Y. Acupuncture reduces apoptosis of granulosa cells in rats with premature ovarian failure via restoring the PI3K/Akt signaling pathway. Int J Mol Sci 2019; 20: 6311.
[22] McLean AC, Valenzuela N, Fai S and Bennett SA. Performing vaginal lavage, crystal violet staining, and vaginal cytological evaluation for mouse estrous cycle staging identification. J Vis Exp 2012; e4389.
[23] Vichinsartvichai P and Sirirat S. Hematologic parameters as the predictors for metabolic syndrome in perimenopausal and postmenopausal women living in urban area: a preliminary report. Prz Menopauzalny 2016; 15: 90-5.
[24] Dougan MM, Hankinson SE, Vivo ID, Tworoger SS, Glynn RJ and Michels KB. Prospective study of body size throughout the life-course and the incidence of endometrial cancer among premenopausal and postmenopausal women. Int J Cancer 2015; 137: 625-637.
[25] Takahashi A, Yousif A, Hong L and Chefetz I. Premature ovarian insufficiency: pathogenesis and therapeutic potential of mesenchymal stem cell. J Mol Med (Berl) 2021; 99: 637-650.
[26] Hopkins AL. Network pharmacology: the next paradigm in drug discovery. Nat Chem Biol 2008; 4: 682-690.
[27] Liang C, Tan S, Huang Q, Lin J, Lu Z and Lin X. Pratensein ameliorates β-amyloid-induced cognitive impairment in rats via reducing oxidative damage and restoring synapse and BDNF levels. Neurosci Lett 2015; 592: 48-53.
[28] Lim H, Park BK, Shin SY, Kwon YS and Kim HP. Methyl caffeate and some plant constituents inhibit age-related inflammation: effects on senescence-associated secretory phenotype (SASP) formation. Arch Pharm Res 2017; 40: 524-535.
[29] Liu J, Shi JL, Guo JY, Chen Y, Ma XJ, Wang SN, Zheng ZQ, Lin MX and He S. Anxiolytic-like effect of Suanzaoren-Wuweizi herb-pair and evidence for the involvement of the monoaminergic system in mice based on network pharmacology. BMC Complement Med Ther 2023; 23: 7.
[30] Liang X, Yan Z, Ma W, Qian Y, Zou X, Cui Y, Liu J and Meng Y. Peroxiredoxin 4 protects against ovarian ageing by ameliorating D-galactose-induced oxidative damage in mice. Cell Death Dis 2020; 11: 1053.
[31] Ko CH, Shen SC, Hsu CS and Chen YC. Mitochondrial-dependent, reactive oxygen species-independent apoptosis by myricetin: roles of protein kinase C, cytochrome c, and caspase cascade. Biochem Pharmacol 2005; 69: 913-927.
[32] Wang Y, Wu JZ, Li Y and Qi X. Polysaccharides of *fructus corni* improve ovarian function in mice with aging-associated perimenopause symptoms. Evid Based Complement Alternat Med 2019; 2019: 2089586.
[33] Zhang S, Zhou HF, Liu YN, Liu B, Yuan YZ, Shan JJ and Ji JJ. Modified Dihuang decoction improves ovarian reserve in mice by regulating Bcl-2-related mitochondrial apoptosis pathway. Zhongguo Zhong Yao Za Zhi 2021; 46: 6493-6501.
[34] Cao LH, Qiao JY, Huang HY, Fang XY, Zhang R, Miao MS and Li XM. PI3K-AKT signaling activa-

tion and icariin: the potential effects on the perimenopausal depression-like rat model. Molecules 2019; 24: 3700.
[35] Shang Z, Fan M, Zhang J, Wang Z, Jiang S and Li W. Red ginseng improves d-galactose-induced premature ovarian failure in mice based on network pharmacology. Int J Mol Sci 2023; 24: 8210.
[36] Zhang F, Cao J, Zhang X, Wang J and Yi X. Efficacy of self-made Gengnian decoction on phosphatidylinositol 3-kinases/protein kinase B/mammalian target of rapamycin signaling pathway in perimenopausal rats. J Tradit Chin Med 2019; 39: 861-866.
[37] Aman Y, Schmauck-Medina T, Hansen M, Morimoto RI, Simon AK, Bjedov I, Palikaras K, Simonsen A, Johansen T, Tavernarakis N, Rubinsztein DC, Partridge L, Kroemer G, Labbadia J and Fang EF. Autophagy in healthy aging and disease. Nat Aging 2021; 1: 634-650.
[38] Tabibzadeh S. Role of autophagy in aging: the good, the bad, and the ugly. Aging Cell 2023; 22: e13753.
[39] Choi JY, Jo MW, Lee EY, Yoon BK and Choi DS. The role of autophagy in follicular development and atresia in rat granulosa cells. Fertil Steril 2010; 93: 2532-2537.
[40] Vilser C, Hueller H, Nowicki M, Hmeidan FA, Blumenauer V and Spanel-Borowski K. The variable expression of lectin-like oxidized low-density lipoprotein receptor (LOX-1) and signs of autophagy and apoptosis in freshly harvested human granulosa cells depend on gonadotropin dose, age, and body weight. Fertil Steril 2010; 93: 2706-2715.
[41] Jiang Y, Wang H, Yu X and Ding Y. Lycium barbarum polysaccharides regulate AMPK/Sirt autophagy pathway to delay D-gal-induced premature ovarian failure. Zhongguo Zhong Yao Za Zhi 2022; 47: 6175-6182.